Pergamon

Int. J. Solids Structures Vol. 32, No. 24, pp. 3537–3554, 1995

0020-7683/95 $9.50 + .00

0020-7683(95)00008-9

SOLUTIONS OF THERMOELASTIC CRACK PROBLEMS IN BONDED DISSIMILAR MEDIA OR HALF-PLANE MEDIUM

C. K. CHAO and M. H. SHEN
Department of Mechanical Engineering, National Taiwan Institute of Technology, Taipei, Taiwan, 106, Republic of China

(*Received* 13 *May* 1994 ; *in revised form* 13 *February* 1995)

Abstract— The two-dimensional thermoelastic crack problem in bonded dissimilar media or in a half-plane medium is considered. The proposed method for solving this problem consists of two parts. In the first part, complex potential functions are derived which are enforced to satisfy the continuity conditions across the interface, while the second part consists of the derivation of singular integral equations by introducing the dislocation functions along the crack border which are solved numerically. For both half-plane and two bonded half-plane problems associated with an insulated crack, the thermal stress intensity factors are computed numerically by using the appropriate interpolation formulae. The results compared with those of the homogeneous case given in the literature show that the method proposed here is effective, simple and general.

1. INTRODUCTION

Boundary value problems involving cracks in plane elasticity and/or thermoelasticity have been widely solved by many researchers. One of the most widely used methods in solving crack problems is based on the application of complex variables in conjunction with the continuation technique which reduces the mixed boundary value problem to a Riemann–Hilbert problem for a sectionally holomorphic function. The theory of complex variables provides the most rigorous method for solving two-dimensional elasticity and/or thermoelasticity problems. However, the closed form solutions are only available for some specific problems. It is known that where the crack problem is associated with at least one separate boundary surface, it is impossible to achieve a closed form solution. For example, for the problem containing cracks in a half-plane or two bonded half-plane media there is no closed form solution available. An alternative method for solving such complicated crack problems may be formulated in terms of a system of singular integral equations by using the related *Green's* function (such as dislocation or concentrated force solution) in conjunction with the technique of superposition. This method has clear advantages in solving the problem by applying a numerical treatment. In the derivation of singular integral equations, the selection of the auxiliary function determines whether the kernels have weak or strong singularities. The kernel with Cauchy-type singularity has been widely used to solve many crack problems which can be reduced to a system of algebraic equations. The numerical results are obtained by applying appropriate orthogonal polynomials. The literature on this subject was collected and summarized by Erdogan *et al.* (1973). On the other hand, the singular integral equation with a logarithmic singular kernel is also applied frequently to crack problems. Chen and Cheung (1990) solved some elastic half-plane problems by using log-type singular integral equations based on elementary solutions and the principle of superposition. In the present approach, similar to the derivations followed by Chen and Hasebe (1992), the thermoelastic crack problems in bonded dissimilar media and a half-plane medium are solved by taking some density distributions of the potential functions along the crack, which already satisfy the required boundary conditions along the given boundary surface. This is accomplished by establishing interdependent relations of the related complex potential functions based on the analytical continuation theorem. The proposed method takes advantage of automatically satisfying the boundary conditions along the boundary surfaces (free surface or interface) and then leaves the determinations

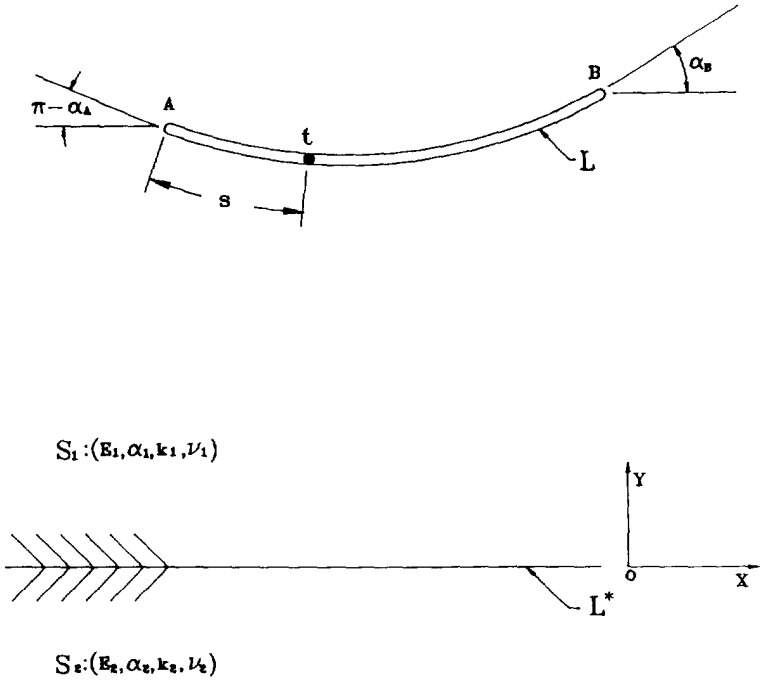

Fig. 1. A curved crack in two bonded dissimilar materials.

of unknown coefficients of the potential functions along the crack surfaces which may be solved numerically in a straightforward manner. The relationships of interdependent functions derived in the present study can also be reduced directly to the corresponding half-plane and homogeneous problems. Both two bonded half-plane and half-plane problems associated with a single curved crack (or line crack) under a remote heat flux are given to illustrate the use of the present approach. The results associated with the thermoelastic homogeneous problem containing a single crack are also provided to compare the given exact solutions for demonstrating the flexibility and the accuracy of the present study.

2. COMPLEX POTENTIAL FORMULATIONS

2.1. *Analytical continuation*

For two-dimensional steady state heat conduction problems, the temperature functions associated with bi-material media can be obtained from two complex potentials $\theta_1(z)$ and $\theta_2(z)$ which satisfy the Laplace equation within the domains S_1 and S_2 (Fig. 1) respectively (Ozisik, 1980). In order to formulate the boundary conditions, the resultant heat flux Q_j and temperature T_j for each medium are expressed in terms of the complex potential as follows

$$Q_j = \int (q_{xj}\,dy - q_{yj}\,dx) = -k_j \operatorname{Im}[\theta_j(z)] \tag{1}$$

$$T_j = \operatorname{Re}[\theta_j(z)] \tag{2}$$

where Re and Im denote the real and imaginary parts of the bracketed expression, respectively. The quantities q_{xj}, q_{yj} in eqn (1) are the components of heat flux in the x- and y-directions, respectively, and k_j stands for the heat conductivity with $j = 1$ for S_1 and $j = 2$ for S_2.

If there exists a curved crack (or line crack) L in one of the two dissimilar media, say S_1, it is convenient to express the complex potential $\theta_1(z)$ as the combination of θ_{1p} and θ_{1c} which are referred to as the principal and complementary parts of the complex potential,

respectively. Since the temperature and resultant heat flux are continuous across the interface L^*, it implies

$$[\theta_1(t)+\theta_1(t)]^+ = [\theta_2(t)+\bar{\theta}_2(t)] \quad , t\in L^* \tag{3}$$

$$k_1[\theta_1(t)-\theta_1(t)]^+ = k_2[\theta_2(t)-\bar{\theta}_2(t)] \quad , \quad t\in L^* \tag{4}$$

where a bar will be used to indicate a conjugate complex quantity while superscripts + and − are used for the boundary values of the physical quantities as L^* is approached from S_1 and S_2, respectively. It is easy to verify that eqns (3) and (4) are satisfied by the following complex potentials

$$\theta_1(z) = \theta_{1p}(z)+\frac{k_1-k_2}{k_1+k_2}\bar{\theta}_{1p}(z), \quad z\in S_1+L^* \tag{5}$$

$$\theta_2(z) = \frac{2k_1}{(k_1+k_2)}\theta_{1p}(z), \quad z\in S_2+L^*. \tag{6}$$

Once the principal part of the complex potential, $\theta_{1p}(z)$, is determined, the temperature functions associated with the bi-material problem can be obtained by means of eqns (5) and (6).

For two-dimensional isotropic thermoelastic problems, resultant forces and displacements can be expressed as follows (Bogdanoff, 1954)

$$-Y_j+iX_j = \phi_j(z)+z\bar{\phi}_j'(\bar{z})+\bar{\psi}_j(\bar{z}) \tag{7}$$

$$2G_j(u+iv_j) = \kappa_j\phi_j(z)-z\bar{\phi}_j'(\bar{z})-\bar{\psi}_j(\bar{z})+2G_j\beta_j g_j(z)$$

$$g_j(z) = \int\theta_j(z)\,dz \quad (j=1,2) \tag{8}$$

where G_j is the shear modulus, and $\kappa_j=(3-\nu_j)/(1+\nu_j)$, $\beta_j=\alpha_j$ for plane stress and $\kappa_j=3-4\nu_j$, $\beta_j=(1+\nu_j)\alpha_j$ for plane strain, ν_j is Poisson's ratio, α_j being the thermal expansion coefficients. Similar to the previous approach, the complex potentials pertaining to S_1 and S_2 are denoted by $\phi_1(z)$, $\psi_1(z)$ and $\phi_2(z)$, $\psi_2(z)$, respectively and the first two can be divided into two parts, i.e.

$$\phi_1(z) = \phi_{1p}(z)+\phi_{1c}(z), \quad \psi_1(z) = \psi_{1p}(z)+\psi_{1c}(z). \tag{9}$$

Substituting eqn (9) into eqns (7) and (8) to enforce continuity of tractions and displacements across the interface L^*, resulting in :

$$\{\phi_{1p}(t)+\phi_{1c}(t)+[t\bar{\phi}_{1p}'(t)+\bar{\psi}_{1p}(t)]+[t\bar{\phi}_{1c}'(t)+\bar{\psi}_{1c}(t)]\}^+ = \{\phi_2(t)+t\bar{\phi}_2'(t)+\bar{\psi}_2(t)\}^- \tag{10}$$

and

$$\{\kappa_1G_2[\phi_{1p}(t)+\phi_{1c}(t)]-G_2[t\bar{\phi}_{1p}'(t)+\bar{\psi}_{1p}(t)]-G_2[t\bar{\phi}_{1c}'(t)+\bar{\psi}_{1c}(t)]$$
$$+2G_1G_2\beta_1g_1(t)\}^+ = \{\kappa_2G_1\phi_2(t)-G_1[t\bar{\phi}_2'(t)+\bar{\psi}_2(t)]+2G_1G_2\beta_2g_2(t)\}^-. \tag{11}$$

By applying the continuation theorem, eqns (10) and (11) can be used to define the functions $\phi_2(z)$ and $z\bar{\phi}_{1c}'(z)+\bar{\psi}_{1c}(z)$ in terms of ϕ_{1p}, $g_1(z)$, and $g_2(z)$ as follows

$$\phi_2(z) = (1+\gamma_1)\phi_{1p}(z)+\gamma_2 g_{1p}(z)+\gamma_3 g_2(z), \quad z\in S_2+L^* \tag{12}$$

$$z\overline{\phi'_{1c}}(z)+\bar{\psi}_{1c}(z) = \gamma_1\phi_{1p}(z)+\gamma_2 g_{1p}(z)+\gamma_3 g_2(z), \quad z\in S_2+L^* \tag{13}$$

with

$$\gamma_1 = \frac{\alpha+\beta}{1-\beta}, \quad \gamma_2 = \frac{2G_1G_2\beta_1}{G_2+\kappa_2 G_1}, \quad \gamma_3 = -\frac{2G_1G_2\beta_2}{G_2+\kappa_2 G_1}$$

where α and β are the Dundurs constants defined by

$$\alpha = \frac{G_2(1+\kappa_1)-G_1(1+\kappa_2)}{G_2(1+\kappa_1)+G_1(1+\kappa_2)}, \quad \beta = \frac{G_2(\kappa_1-1)-G_1(\kappa_2-1)}{G_2(1+\kappa_1)+G_1(1+\kappa_2)}.$$

Similarly, the functions $\bar{\phi}_{1c}(z)$ and $z\phi'_2(z)+\psi_2(z)$ can be defined as

$$\bar{\phi}_{1c}(z) = \gamma_4[z\phi'_{1p}(z)+\psi_{1p}(z)]+\frac{2G_1G_2\beta_1}{G_1+\kappa_1 G_2}\frac{k_2-k_1}{k_1+k_2}g_{1p}(z), \quad z\in S_2+L^* \tag{14}$$

$$z\phi'_2(z)+\psi_2(z) = (1+\gamma_4)[z\phi'_{1p}+\psi_{1p}(z)]+\frac{2G_1G_2\beta_1}{G_1+\kappa_1 G_2}\frac{k_2-k_1}{k_1+k_2}g_{1p}(z), \quad z\in S_2+L^* \tag{15}$$

where

$$\gamma_4 = \frac{\alpha-\beta}{1+\beta}.$$

After rearrangement, the results of the foregoing manipulations can be summarized as

$$\phi_1(z) = \phi_{1p}(z)+\gamma_4[z\overline{\phi'_{1p}}(z)+\overline{\psi_{1p}}(z)]+\frac{2G_1G_2\beta_1}{G_1+\kappa_1 G_2}\frac{k_2-k_1}{k_1+k_2}\bar{g}_{1p}(z), \quad z\in S_1+L^* \tag{16}$$

$$\psi_1(z) = \psi_{1p}(z)+\gamma_1\bar{\phi}_{1p}(z)-z\phi'_{1c}(z)+\frac{2G_1G_2\beta_1}{\kappa_2 G_1+G_2}\bar{g}_{1p}(z)-\frac{2G_1G_2\beta_2}{\kappa_2 G_1+G_2}\bar{g}_2(z), \quad z\in S_1+L^* \tag{17}$$

$$\phi_2(z) = (1+\gamma_1)\phi_{1p}(z)+\frac{2G_1G_2\beta_1}{\kappa_2 G_1+G_2}g_{1p}(z)-\frac{2G_1G_2\beta_2}{\kappa_2 G_1+G_2}g_2(z), \quad z\in S_2+L^* \tag{18}$$

$$\psi_2(z) = (1+\gamma_4)[z\phi'_{1p}(z)+\psi_{1p}(z)]-z\phi'_2(z)+\frac{2G_1G_2\beta_1}{G_1+\kappa_1 G_2}\frac{k_2-k_1}{k_1+k_2}g_{1p}(z), \quad z\in S_2+L^*. \tag{19}$$

Equations (5) and (6), and eqns (16)–(19) give the general solutions to the thermoelastic bi-material problem provided that the complex potentials θ_{1p}, ϕ_{1p} and ψ_{1p} are appropriately solved.

If one lets $k_1 = k_2$, $G_1 = G_2$, $\kappa_1 = \kappa_2$, and $\beta_1 = \beta_2$ in the above equations, the foregoing results may reduce to

$$\theta_1(z) = \theta_2(z) = \theta_{1p}(z) \tag{20}$$

and

$$\phi_1(z) = \phi_2(z) = \phi_{1p}(z), \quad \psi_1(z) = \psi_2(z) = \psi_{1p}(z), \tag{21}$$

which are the solutions corresponding to the thermoelastic homogeneous problem. Furthermore, if one lets $k_2 = G_2 = 0$, the foregoing results become

$$\theta_1(z) = \theta_{1p}(z) + \theta_{1p}(z) \tag{22}$$

and

$$\phi_1(z) = \phi_{1p}(z) - [z\bar{\phi}'_{1p}(z) + \bar{\psi}_{1p}(z)] \tag{23}$$

$$\psi_1(z) = \psi_{1p}(z) - \bar{\phi}_{1p}(z) + z[\bar{\phi}'_{1p}(z) + z\bar{\phi}''_{1p}(z) + \bar{\psi}'_{1p}(z)] \tag{24}$$

which are the solutions corresponding to the thermoelastic half-plane problem.

2.2. *Integral representation*

Consider a curved crack L to be situated in the upper half-plane, S_1, of an isotropic homogeneous medium (Fig. 1), the corresponding complex potentials can be expressed as

$$\theta_{1p}(z) = -\frac{i}{2\pi}\int_L b_0(s)\log(z-t)\,\mathrm{d}s \tag{25}$$

$$\phi_{1p}(z) = \frac{iG_1}{\pi(1+\kappa_1)}\int_L [b_1(s)+ib_2(s)]\log(z-t)\,\mathrm{d}s \tag{26}$$

$$\psi_{1p}(z) = \frac{-iG_1}{\pi(1+\kappa_1)}\int_L [b_1(s)-ib_2(s)]\log(z-t)\,\mathrm{d}s - \frac{iG_1}{\pi(1+\kappa_1)}\int_L \frac{[b_1(s)+ib_2(s)]\bar{t}}{z-t}\mathrm{d}s \tag{27}$$

where $b_0(s)$ indicates the strength of the temperature dislocation and $b_1(s)$, $b_2(s)$ indicate the components of the displacement discontinuities across the dislocation line. Substituting eqn (25) into eqns (5) and (6), the temperature potentials are found as

$$\theta_1(z) = -\frac{i}{2\pi}\int_L b_0(s)\log(z-t)\,\mathrm{d}s + \frac{(k_1-k_2)}{2\pi(k_1+k_2)}\left[i\int_L b_0(s)\log(z-\bar{t})\,\mathrm{d}s\right] \tag{28}$$

$$\theta_2(z) = -\frac{k_1}{\pi(k_1+k_2)}\left[i\int_L b_0(s)\log(z-t)\,\mathrm{d}s\right]. \tag{29}$$

In the present study, the unknown function $b_0(s)$ will be obtained on the basis that the total heat flux across the crack surface L must be balanced by the given resultant heat fluxes Q_1 across L, i.e.

$$Q_1 = \int_L (q_{x1}\,\mathrm{d}y - q_{y1}\,\mathrm{d}x) = -k_1\,\mathrm{Im}[\theta_1(t)] + c_0, \quad t \in L \tag{30}$$

where c_0 is a constant. In addition, the single-valued condition of the temperature must be satisfied, i.e.

$$\int_L b_0(s)\,\mathrm{d}s = 0. \tag{31}$$

Now, the substitution of eqn (28) into eqn (30) yields the singular integral equation subject to the subsidiary condition, eqn (31), which may be solved numerically. Once the

temperature functions are given, the complex potentials $\phi_1(z)$ and $\psi_1(z)$ can be obtained by substituting eqns (26)–(29) into eqns (16) and (17) and performing the integration $g_j(z) = \int \theta_j(z)\,dz$, resulting in

$$\phi_1(z) = \frac{iG_1}{\pi(1+\kappa_1)}\int_L [b_1(s)+ib_2(s)]\log(z-t)\,ds + \gamma_4\frac{iG_1}{\pi(1+\kappa_1)}\left\{\int_L -\frac{z[b_1(s)-ib_2(s)]}{z-\bar{t}}\,ds + \int_L [b_1(s)+ib_2(s)]\log(z-\bar{t})\,ds + \int_L \frac{[b_1(s)-ib_2(s)]t}{z-\bar{t}}\,ds\right\} + \frac{2G_1G_2\beta_1}{\kappa_1G_2+G_1}\frac{i}{2\pi}\frac{k_2-k_1}{k_1+k_2}\int_L b_0(s)[(z-\bar{t})\log(z-\bar{t})-z]\,ds \tag{32}$$

$$\psi_1(z) = \frac{-iG_1}{\pi(1+\kappa_1)}\int_L [b_1(s)-ib_2(s)]\log(z-t)\,ds - \frac{iG_1}{\pi(1+\kappa_1)}\int_L \frac{[b_1(s)+ib_2(s)]\bar{t}}{z-t}\,ds + \gamma_4\frac{-iG_1}{\pi(1+\kappa_1)}\int_L [b_1(s)-ib_2(s)]\log(z-\bar{t})\,ds + \gamma_4\frac{iG_1}{\pi(1+\kappa_1)}\left\{\int_L \frac{z[b_1(s)-ib_2(s)]}{z-\bar{t}}\,ds - \left[\int_L \frac{z^2[b_1(s)-ib_2(s)]}{(z-\bar{t})^2}\,ds + \int_L \frac{z[b_1(s)+ib_2(s)]}{z-\bar{t}}\,ds - \int_L \frac{z[b_1(s)-ib_2(s)]t}{(z-\bar{t})^2}\,ds\right]\right\} + \frac{2G_1G_2\beta_1}{\kappa_2G_1+G_2}\frac{i}{2\pi}\left\{\int_L b_0(s)[(z-\bar{t})\log(z-\bar{t})-z]\,ds - \frac{2k_1\beta_2}{(k_1+k_2)\beta_1}\int_L b_0(s)[(z-\bar{t})\log(z-\bar{t})-z]\,ds\right\}. \tag{33}$$

The unknown functions $b_1(s)$ and $b_2(s)$ appearing in eqns (32) and (33) will be obtained on the basis that the force acting on the crack surface must be balanced by the given resultant force applied on the crack surface, i.e.

$$-Y_1 + iX_1 = \phi_1(t) + z\overline{\phi_1'(t)} + \overline{\psi_1(t)} + c_1 + ic_2, \quad t \in L \tag{34}$$

where c_1 and c_2 are real constants. Substituting eqns (32) and (33) into eqn (34) leads to the singular integral equation together with the subsidiary condition

$$\int_L [b_1(s)+ib_2(s)]\,ds - \int_L \beta_1\left[B_0(s)\frac{dt}{ds}\right]ds = 0 \tag{35}$$

where

$$B_0(s) = \int b_0(\xi)\,d\xi.$$

which is the requirement for a single-valued displacement.

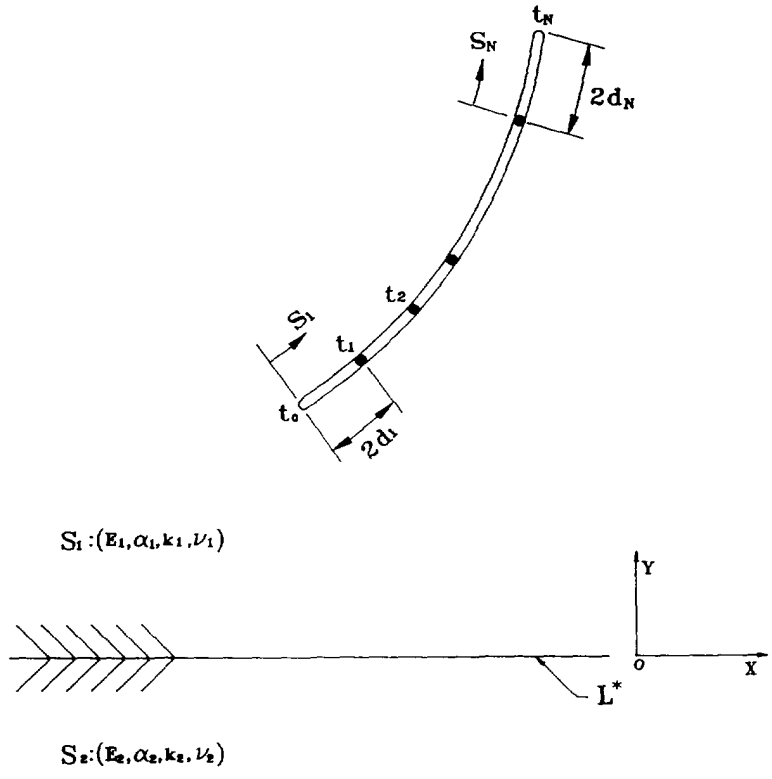

Fig. 2. Division and nodal distribution for the curved crack.

3. NUMERICAL SOLUTIONS

The dislocation functions appearing in the singular integral equations (30) and (34) observing the subsidiary conditions, eqns (31) and (35) will be solved numerically using the appropriate interpolation formulae. In order to perform the numerical calculation, the curved crack (or line crack) is approximated by N line segments as indicated in Fig. 2. Since the temperature dislocation distribution $b_0(s)$ and displacement distributions $b_1(s)$, $b_2(s)$ contain square-root singularity at the vicinity of the crack tip, the interpolation formulae in local coordinates s_1 and s_N for each crack tip element are defined as (Chen and Cheung, 1990)

$$b_i(s_1) = b_{i,0}\left(\sqrt{\frac{2d_1}{s_1}} - 1\right) + b_{i,1} \quad (i = 0, 1, 2) \tag{36}$$

and

$$b_i(s_N) = b_{i,N}\left(\sqrt{\frac{2d_N}{2d_N - s_N}} - 1\right) + b_{i,N-1} \quad (i = 0, 1, 2). \tag{37}$$

Meanwhile, the interpolation formulae for the intermediate segments in local coordinates $s_j (2 \leqslant j \leqslant N-1)$ are taken as (Chen and Cheung, 1990)

$$b_i(s_j) = b_{i,j-1}\frac{2d_j - s_j}{2d_j} + b_{i,j}\frac{s_j}{2d_j} \quad (i = 0, 1, 2) \tag{38}$$

where $d_j (1 < j < N)$ are the half length for each line segment and $b_{i,j} (0 \leqslant j \leqslant N)$ are the unknown coefficients to be determined. If the above formulae are used, the integral equation (30) together with the subsidiary condition (31), can be carried out to yield $N+2$ algebraic

Table 1. Comparisons between the calculated and exact values of the thermal stress intensity factors for different discretization (N)

N	$K_{IA}/(K_{II})_{exact}$	$K_{IB}/(K_{II})_{exact}$	$K_{IIA}/(K_{II})_{exact}$	$K_{IIB}/(K_{II})_{exact}$
10	0.0000	0.0000	0.9919	−0.9919
20	0.0000	0.0000	0.9982	−0.9982
30	0.0000	0.0000	0.9999	−0.9999

equations for $N+2$ unknown coefficients. Similarly, the integral equation (34) together with the subsidiary condition (35), can be solved to yield $2N+4$ algebraic equations for $2N+4$ unknown constants. The thermal stress intensity factors at two crack tips are directly related to the coefficients $b_{1,0}$, $b_{2,0}$ and $b_{1,N}$, $b_{2,N}$ by (Chen and Cheung, 1990)

$$K_{IA}-iK_{IIA}=(2\pi)^{3/2}(2d_1)^{1/2}\exp(-i\alpha_A)\frac{iG_1}{\pi(1+\kappa_1)}(b_{1,0}+ib_{2,0}) \tag{39}$$

and

$$K_{IB}-iK_{IIB}=(2\pi)^{3/2}(2d_N)^{1/2}\exp(-i\alpha_B)\frac{iG_1}{\pi(1+\kappa_1)}(b_{1,N}+ib_{2,N}) \tag{40}$$

where the angles α_A and α_B are defined in Fig. 1.

3.1. *Homogeneous problem*

For the purpose of examining the accuracy of the present approach, the calculated stress intensity factors of two numerical examples associated with the thermoelastic homogeneous problem are provided to compare the given exact solutions. First, we consider an insulated line crack of length $2l$ in an infinite medium under a remote uniform heat flux, q, in the direction perpendicular to that of a line crack. The exact thermal stress intensity factors at crack tip A for this problem are

$$(K_I)_{exact}=0,\quad (K_{II})_{exact}=\frac{2\beta Gl^{3/2}q\sqrt{\pi}}{(1+\kappa)k}.$$

Comparisons between the calculated and exact values of the thermal stress intensity factors for different numbers of line segment with equally divided space are given in Table 1.

From the above numerical examination, we see that even for a coarse mesh, i.e. $N=10$, the proposed numerical method provides reliable results. Next, we consider an insulated circular-arc crack with the half angle $\theta=30$ and the radius r subject to uniform heat flow q directed at an angle γ with respect to the central axis of an arc crack. The results from Fig. 3 (tip A) and Fig. 4 (tip B) indicate that the calculated values of the stress intensity factors yield good accuracy when compared to the exact results given by Chao and Shen (1993) as the number of line segments $N=30$.

3.2. *Half-plane problem*

As mentioned previously, the solutions associated with the half-plane problem can be retrieved from the results given for the bi-material problem if $k_2=G_2=0$. Referring to Figs 5 and 6, two specific crack configurations associated with a half-plane medium (or two bonded half-plane media) are considered to illustrate the use of the present approach. Note that both the half-plane surface and the crack are assumed to be insulated and traction-free.

3.2.1. *An insulated line crack*. Some numerical calculations are carried out to clarify the effects of the geometrical parameters on the thermal stress intensity factors as shown in

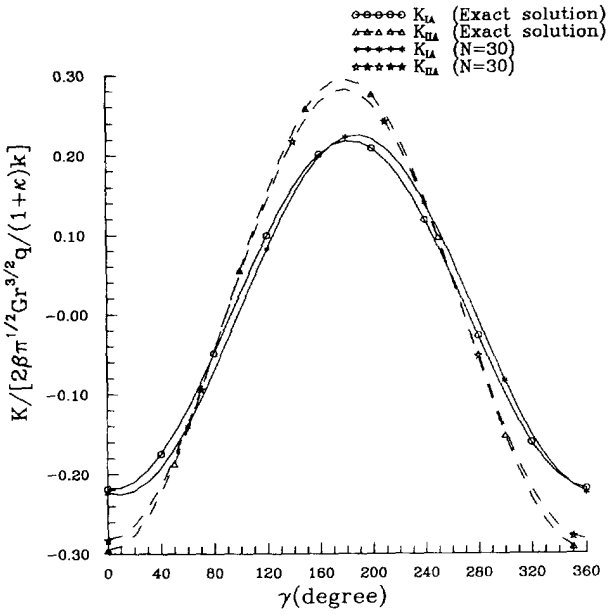

Fig. 3. Comparisons between the calculated and exact values of the thermal stress intensity factors at tip A of the circular-arc crack.

Figs 7 and 8. It is seen that the opening mode stress intensity factors K_I increase monotonically at both crack tips as the insulated line crack approaches the boundary surface of a semi-infinite medium as indicated in Fig. 7, except in the cases of $\lambda = 0^\circ$ and $\lambda = -90^\circ$ where the thermal stress intensity factors for the opening mode are zero. Figure 8 reveals that the distance between a line crack and the boundary surface has a remarkable influence upon the in-plane shear mode stress intensity factors K_{II} at tip-A, particularly for small values of h/l. This is because the presence of an insulated boundary surface may result in the thermal energy cumulation around the crack tip closer to the boundary surface. Notice that the thermal stress intensity factor for the in-plane shear mode is zero for $\lambda = 0^\circ$ since in this case the insulated crack does not disturb the stationary uniform heat flow.

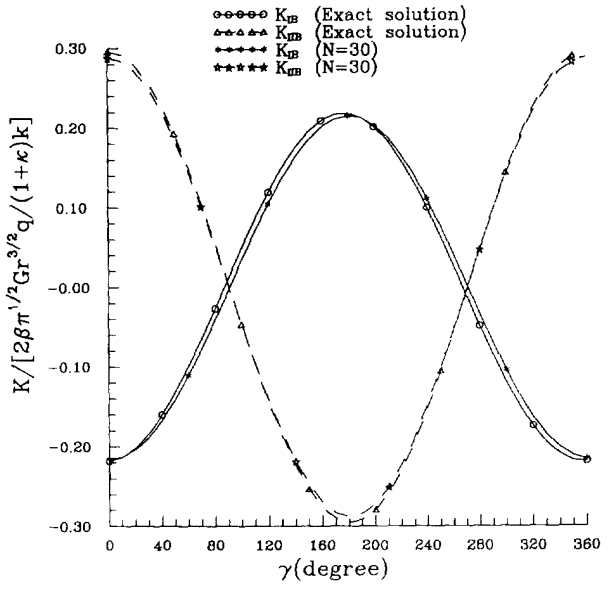

Fig. 4. Comparisons between the calculated and exact values of the thermal stress intensity factors at tip B of the circular-arc crack.

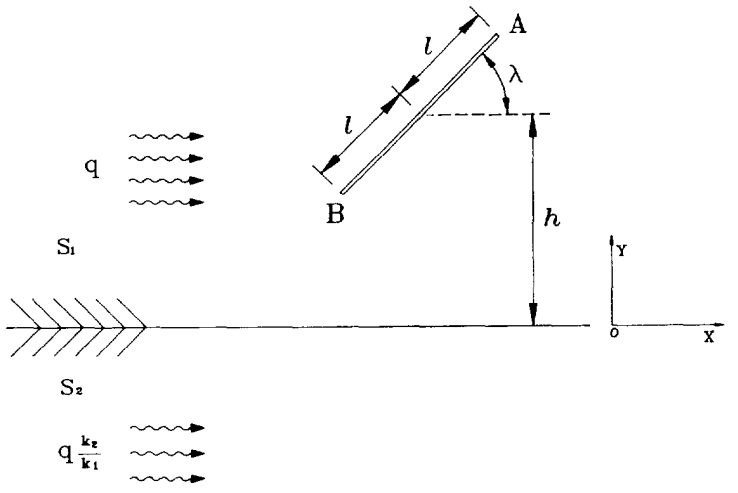

Fig. 5. An insulated line crack in two bonded dissimilar materials.

3.2.2. *An insulated circular-arc crack.* Figures 9 and 10 display the dimensionless stress intensity factors at tip-A for the opening mode and in-plane shear mode, respectively against the half angle θ of the insulated circular-arc crack. As expected, the magnitude of local stresses increases with decreasing distance between the circular-arc crack and the boundary surface. It is interesting to see that the open mode stress intensity factor attains its maximum value around $\theta = 78$ and then decreases as the crack angle further increases. This is because the presence of an insulated crack surface may be able to shield the heat flux as the crack angle extends beyond 78 and then results in decreasing the thermal energy intensification around the crack tips.

3.3. *Two bonded half-plane problem*

Referring to Figs 5 and 6, the line crack and circular-arc crack configurations are considered separately to be situated in the upper portions of dissimilar media. In what follows, k_2/k_1 and β_2/β_1 are fixed at 1 except specifically stated.

3.3.1. *An insulated line crack.* Figure 11 indicates that the positive thermal stress intensity factors increase with a decrease in the distance between a line crack and the interface as the crack is placed in a hard material ($G_2/G_1 = 0.5$). On the other hand, the negative thermal stress intensity factors enhance as a line crack placed in a soft material

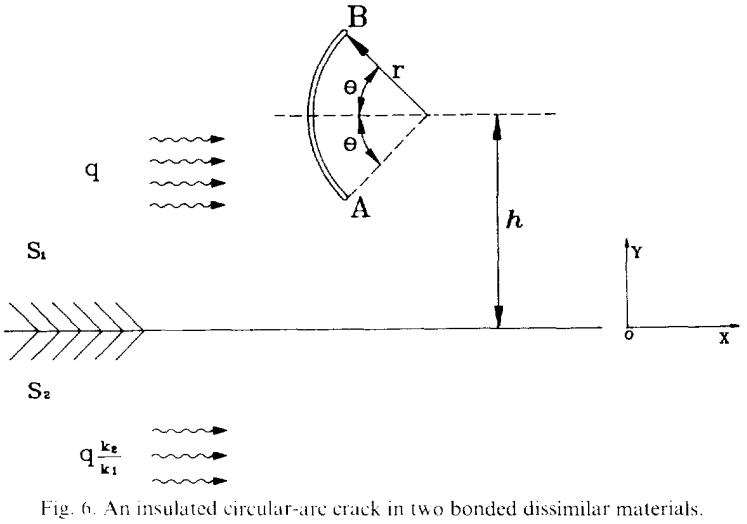

Fig. 6. An insulated circular-arc crack in two bonded dissimilar materials.

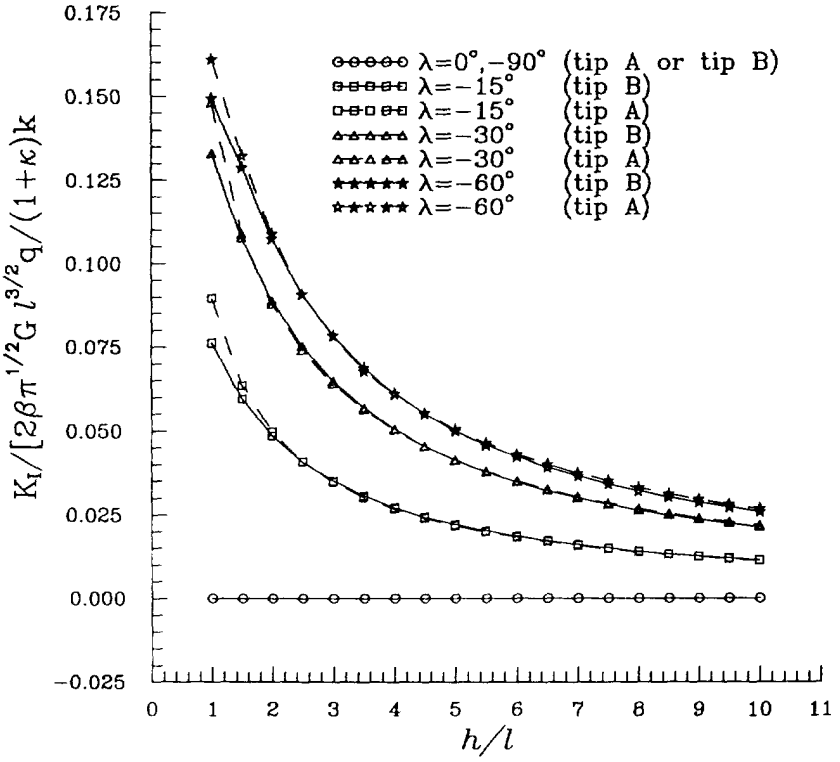

Fig. 7. The mode I stress intensity factors versus the distance from the center of the line crack to the boundary surface of the half-plane medium.

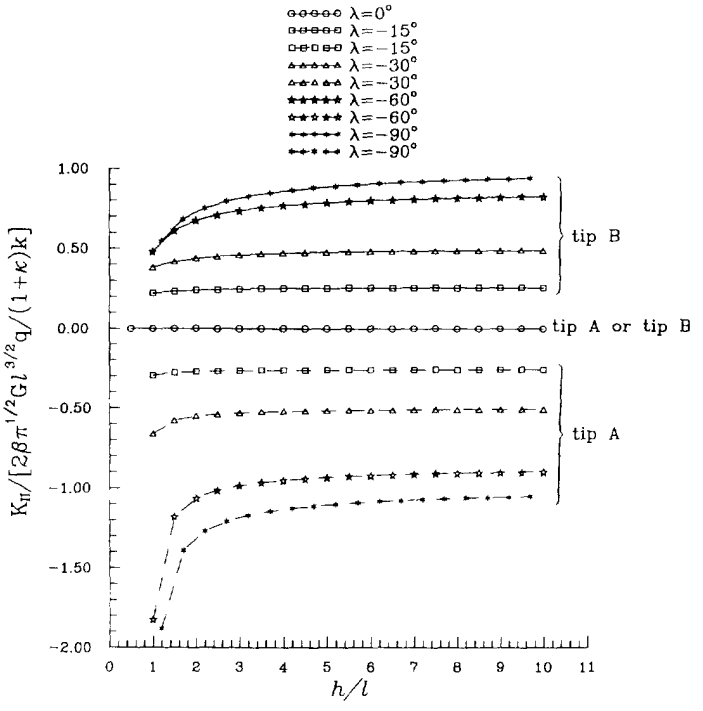

Fig. 8. The mode II stress intensity factors versus the distance from the center of the line crack to the boundary surface of the half-plane medium.

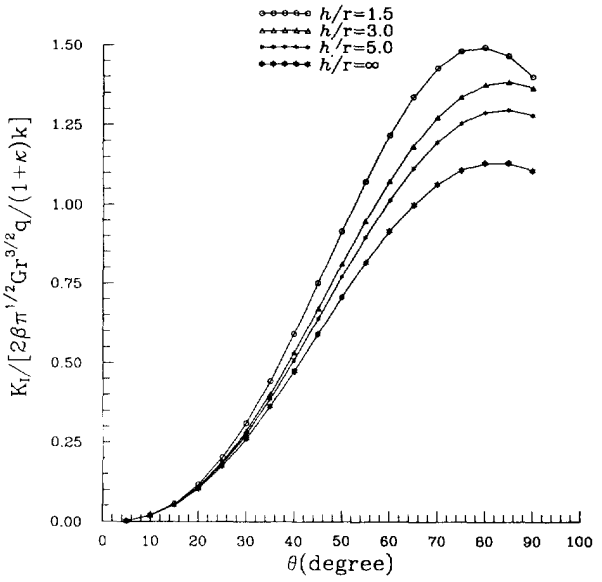

Fig. 9. The mode I stress intensity factors versus the half angle θ of the circular-arc crack in the half-plane medium.

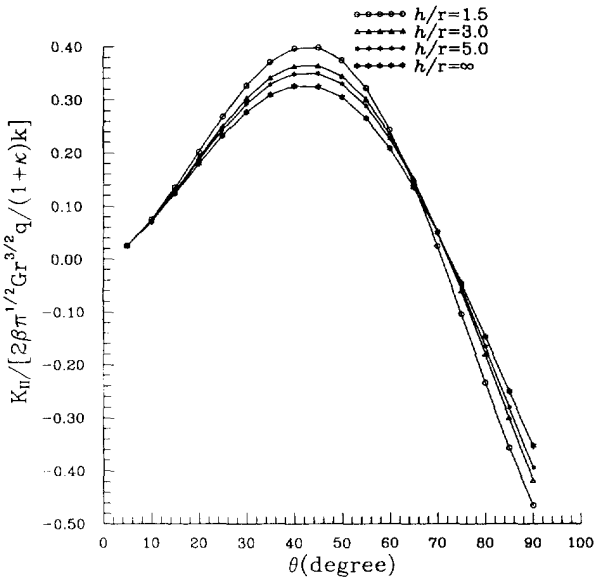

Fig. 10. The mode II stress intensity factors versus the half angle θ of the circular-arc crack in the half-plane medium.

(G_2 G_1 = 3.0) approaches the boundary surface as indicated in Fig. 12. This can be explained by the fact that the stiffer material tends to act as a barrier in load transfer. Note that the open mode stress intensity factor for a crack either parallel or perpendicular to the interface is zero, which is the same as the result given for the half-plane problem. When a heat flow approaches the top medium S_1 from the lower medium S_2 in the direction perpendicular to the interface, the thermal stress intensity factors for a crack perpendicular or parallel to the interface are displayed in Figs 13 and 14. It is seen that both K_I and K_{II} for a crack perpendicular to the interface ($\lambda = 90°$) are found to vanish since the uniform heat flow would not be disturbed by the presence of an insulated crack. On the other hand, thermal stress intensity factors for a crack parallel to the interface ($\lambda = 0°$) do exist and the effect of material rigidity G_2/G_1 on the factors K_I, K_{II} is enhanced, particularly for small values of h/l. The thermal stress intensity factors influenced by the ratio of thermal expansion coefficients β_2/β_1 are displayed in Figs 15 and 16. The results show that positive thermal

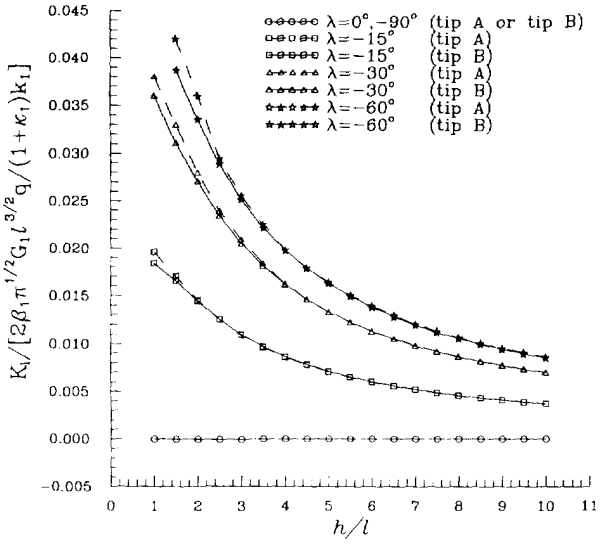

Fig. 11. The mode I stress intensity factors versus the distance from the center of the line crack to the boundary surface of two bonded materials ($G_2/G_1 = 0.5$).

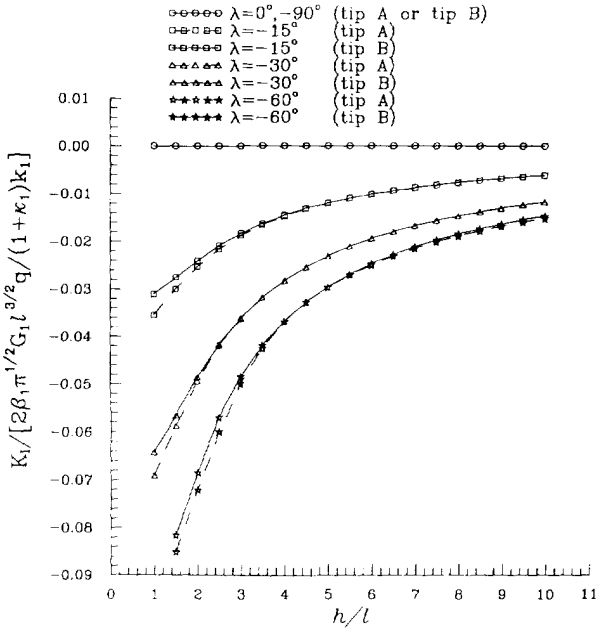

Fig. 12. The mode I stress intensity factors versus the distance from the center of the line crack to the boundary surface of two bonded materials ($G_2/G_1 = 3.0$).

stress intensity factors are exhibited as a crack is placed in a material with a higher thermal expansion coefficient and vice versa. It should be noted that the numerical results of the thermal stress intensity factors are very sensitive to the distance h since the convergence becomes slower as the crack approaches the boundary surface.

3.3.2. *An insulated circular-arc crack.* The effects of material properties and geometrical parameters on the thermal stress intensity factors at tip A for a circular-arc crack problem are exhibited in Figs 17 and 18. The results generally show that both K_I and K_{II} increase with decreasing distance h/r for a crack near an interface where the material next to it is less rigid, which also agrees with the behavior of a crack near the boundary surface of the half-plane problem. On the other hand, the situation reverses for a crack near an interface where the material next to it is more rigid. As a heat flow approaches the top medium S_1 from the lower medium S_2 in the direction perpendicular to the interface, the thermal

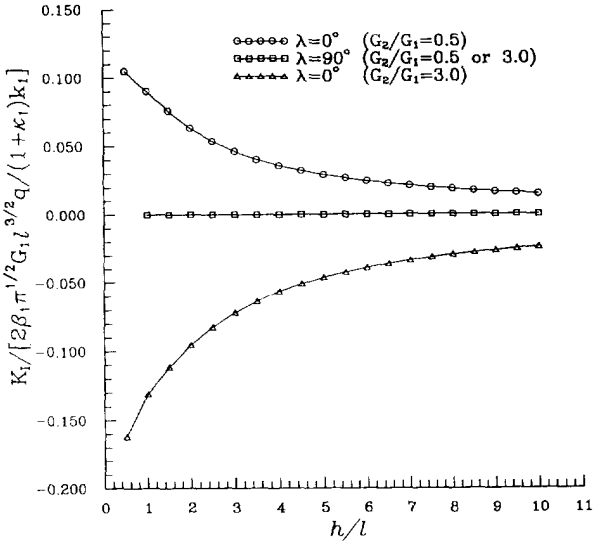

Fig. 13. The mode I stress intensity factors versus the distance from the center of the line crack to the boundary surface of two bonded materials as a heat flux approaches from S_2 to S_1.

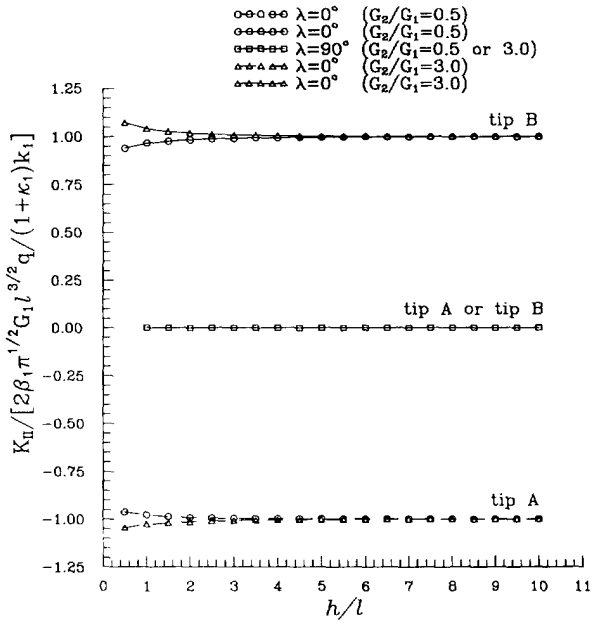

Fig. 14. The mode II stress intensity factors versus the distance from the center of the line crack to the boundary surface of two bonded materials as a heat flux approaches S_1 from S_2.

intensity factors for different ratios of material rigidity and thermal expansion coefficient are displayed in Figs 19–22. It is suggested that the influence of the material rigidity G_2/G_1 on the thermal stress intensity factors is quite similar to the influence of the thermal expansion coefficient β_2, β_1.

4. CONCLUSIONS

A general solution to the thermoelastic crack problem in dissimilar media is presented via the application of the complex variables theory of and the use of dislocation distributions for determining the unknown functions. Based on the analytical continuation theorem, both the temperature and displacement complex potentials are formulated such that the continuity conditions across the interface are satisfied. The resulting singular integral equations with a logarithmic singular kernel are established from the equilibrium conditions

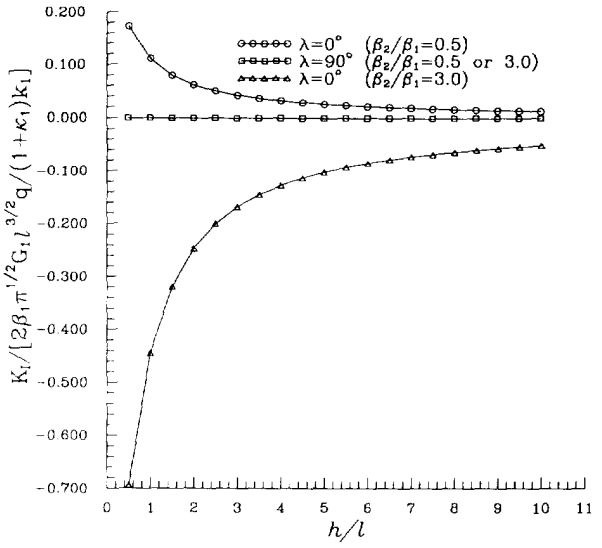

Fig. 15. The mode I stress intensity factors versus the distance from the center of the line crack to the boundary surface of two bonded materials as a heat flux approaches S_1 from S_2 ($G_2/G_1 = 1.0$).

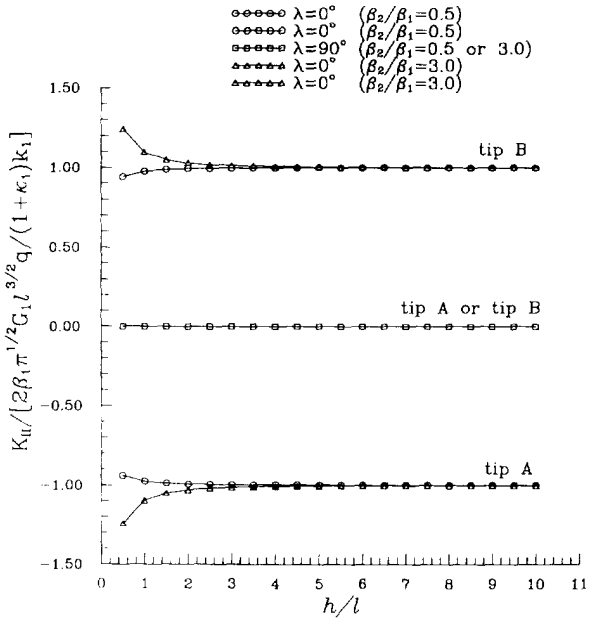

Fig. 16. The mode II stress intensity factors versus the distance from the center of the line crack to the boundary surface of two bonded materials as a heat flux approaches S_1 from S_2 ($G_2/G_1 = 1.0$).

of resultant force and heat flux across the crack surface. This leaves unknown functions (dislocation functions) appearing in the singular integral equations which can then be solved numerically. The thermal stress intensity factors which are directly related to the coefficients of dislocation functions are computed numerically in a straightforward manner. The results are compared to those of the homogeneous case found in the literature which show that the method proposed here is effective, simple and general. Both half-plane and two bonded half-plane problems associated with an insulated circular-arc crack (or line crack) are considered to demonstrate the effects of the geometrical parameters on the strength of the thermal stress singularity. It must be emphasized that the method proposed in the present study can also be applied to solve more complicated problems with irregularly shaped multiple cracks embedded in thermoelastic dissimilar media.

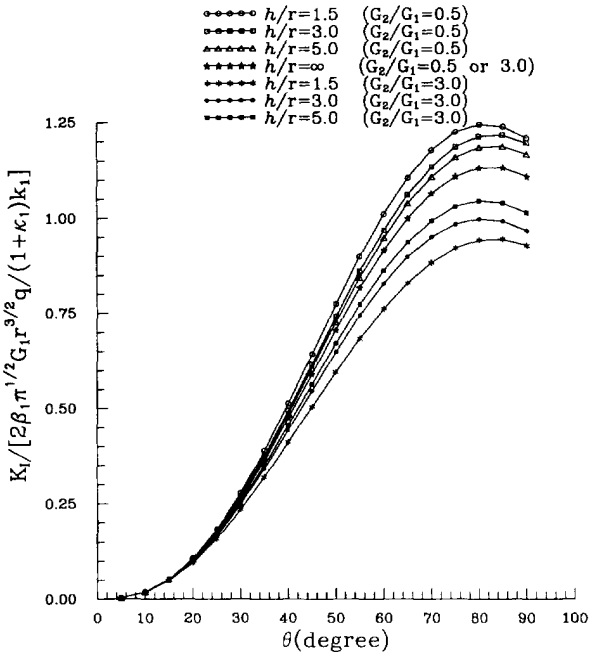

Fig. 17. The mode I stress intensity factors versus the half angle θ of the circular-arc crack in two bonded materials.

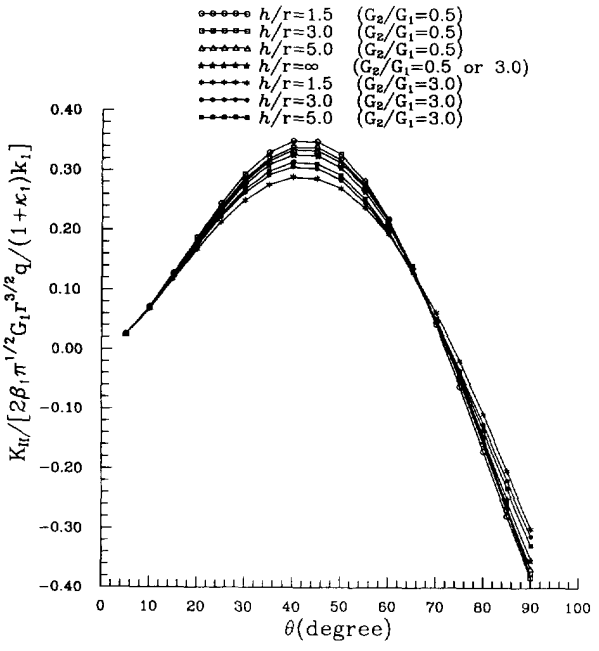

Fig. 18. The mode II stress intensity factors versus the half angle θ of the circular-arc crack in two bonded materials.

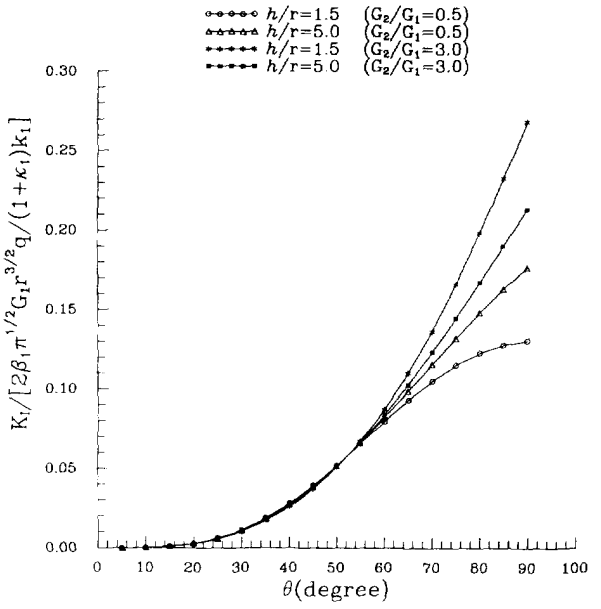

Fig. 19. The mode I stress intensity factors versus the half angle θ of the circular-arc crack in two bonded materials as a heat flux approaches S_1 from S_2.

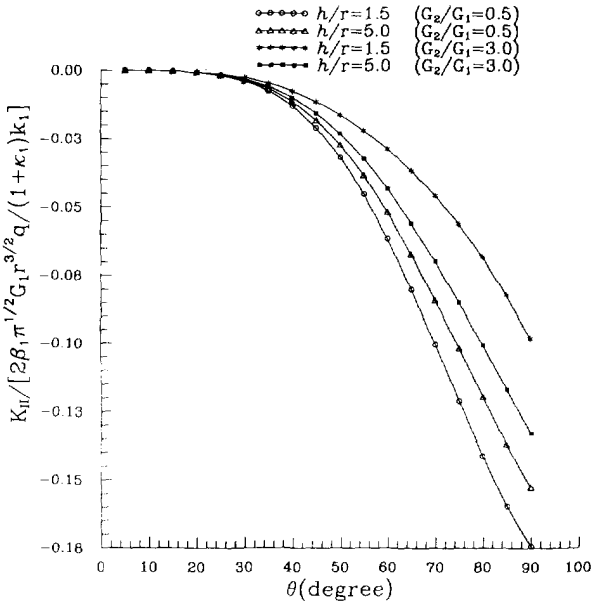

Fig. 20. The mode II stress intensity factors versus the half angle θ of the circular-arc crack in two bonded materials as a heat flux approaches S_1 from S_2.

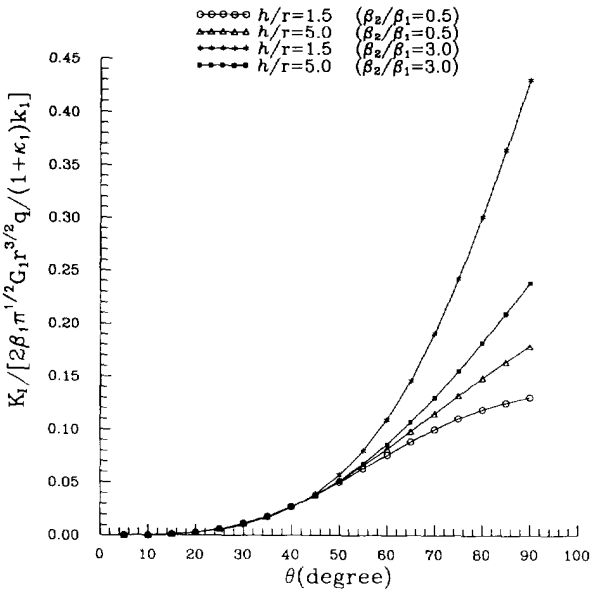

Fig. 21. The mode I stress intensity factors versus the half angle θ of the circular-arc crack in two bonded materials as a heat flux approaches S_1 from S_2 ($G_2/G_1 = 1.0$).

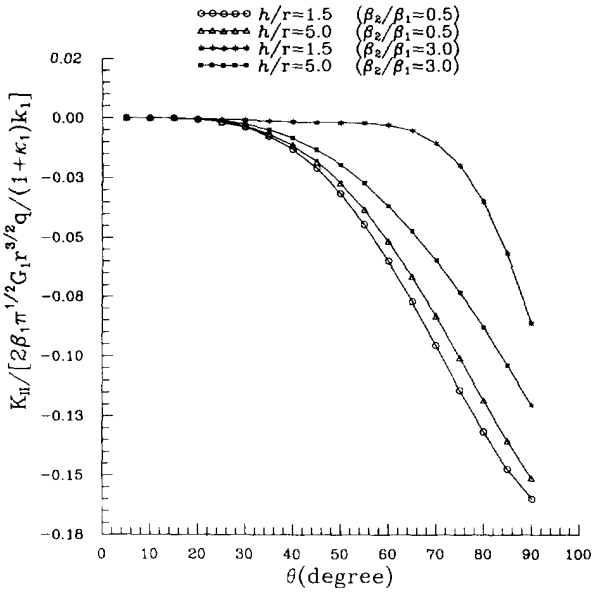

Fig. 22. The mode II stress intensity factors versus the half angle θ of the circular-arc crack in two bonded materials as a heat flux approaches S_1 from S_2 ($G_2/G_1 = 1.0$).

Acknowledgement—The authors would like to thank the support by the National Science Council, Republic of China, through grant No. NSC. 83-0401-E011-003.

REFERENCES

Bogdanoff, J. L. (1954). Note on thermal stress. *J. Appl. Mech.* **21**, 88.

Chao, C. K. and Shen, M. H. (1993). Thermoelastic problem of curvilinear cracks in bonded dissimilar materials. *Int. J. Solids Structures* **30**, 3041–3057.

Chen, Y. Z. and Cheung, Y. K. (1990). New integral equation approach for crack problem in elastic half-plane. *Int. J. Fract. Mech.* **46**, 57–69.

Chen, Y. Z. and Hasebe, N. (1992). Stress-intensity factors for curved circular crack in bonded dissimilar materials. *Theoretical Appl. Fract. Mech.* **17**, 189–196.

Erdogan, F., Gupta, G. D. and Cook, T. S. (1973). Numerical solution of singular integral equations. In *Mechanics of Fracture* 1 (Edited by G. C. Sih). Noordhoff, Leyden.

Ozisik, M. N. (1980). *Heat Conduction*. Wiley, New York.